

Original Article

Expression of the UVR8 photoreceptor in different tissues reveals tissue-autonomous features of UV-B signalling

Péter Bernula¹, Carlos Daniel Crocco², Adriana Beatriz Arongaus², Roman Ulm², Ferenc Nagy^{1,3} & András Viczián¹ 

¹Institute of Plant Biology, Biological Research Centre, Temesvári krt. 62. H-6726 Szeged, Hungary, ²Department of Botany and Plant Biology, Sciences III, University of Geneva, CH-1211 Geneva 4, Switzerland and ³Institute of Molecular Plant Science, School of Biological Sciences, University of Edinburgh, Edinburgh EH9 3JH, UK

ABSTRACT

The Arabidopsis UV-B photoreceptor UV RESISTANCE LOCUS 8 (UVR8) orchestrates the expression of hundreds of genes, many of which can be associated with UV-B tolerance. UV-B does not efficiently penetrate into tissues, yet UV-B regulates complex growth and developmental responses. To unravel to what extent and how UVR8 located in different tissues contributes to UV-B-induced responses, we expressed UVR8 fused to the YELLOW FLUORESCENT PROTEIN (YFP) under the control of tissue-specific promoters in a *uvr8* null mutant background. We show that (1) UVR8 localized in the epidermis plays a major role in regulating cotyledon expansion, and (2) expression of UVR8 in the mesophyll is important to protect adult plants from the damaging effects of UV-B. We found that UV-B induces transcription of selected genes, including the key transcriptional regulator *ELONGATED HYPOCOTYL 5 (HY5)*, only in tissues that express UVR8. Thus, we suggest that tissue-autonomous and simultaneous UVR8 signalling in different tissues mediates, at least partly, developmental and defence responses to UV-B.

Key-words: Arabidopsis; tissue specificity; ultraviolet-B.

INTRODUCTION

Plants must adapt to the environment to optimize growth and development for survival and successful reproduction. Light is an essential environmental factor and necessary not only for photosynthesis but also as a signal for proper development and growth. Plants evolved various photoreceptors that are able to monitor changes in the quantity and quality of the ambient light environment. These include the blue/UV-A light absorbing phototropins, cryptochromes and Zeitlupe family receptors; the red/far-red absorbing phytochromes (phyA-phyE), as well as the UV-B photoreceptor UV RESISTANCE LOCUS 8 (UVR8) (Galvão & Fankhauser, 2015).

UV-B radiation (280–315 nm) is an integral part of sunlight reaching the Earth's surface, as it is only partially absorbed by the stratospheric ozone layer. UV-B can damage several macromolecules (DNA, proteins etc.) (Hollosy, 2002). However, UV-B also activates UVR8-dependent signal transduction pathways and triggers responses that manifest as

inhibition of hypocotyl elongation, reduction of leaf size, entrainment of the circadian clock, modification of shade avoidance response, alteration of phototropism, increased accumulation of photo-protective flavonoids and increased survival under UV-B stress (Kliebenstein *et al.*, 2002; Brown *et al.*, 2005; Favory *et al.*, 2009; Feher *et al.*, 2011; Morales *et al.*, 2013; Hayes *et al.*, 2014; Jenkins, 2014; Vandenbussche *et al.*, 2014).

At the cellular level, the UVR8 photoreceptor can be detected both in the cytoplasm and the nucleus in visible light, but irradiation with UV-B increases accumulation of UVR8 in the nucleus (Kaiserli & Jenkins, 2007; Yin *et al.*, 2016). Nuclear localization of UVR8 is required but not sufficient for UV-B signalling (Brown *et al.*, 2005; Kaiserli & Jenkins, 2007; Yin *et al.*, 2016). It is a matter of debate whether or not UVR8 directly associates with chromatin to regulate UV-B-dependent transcription of target genes, including *HY5* (Cloix & Jenkins, 2008; Binkert *et al.*, 2016). The *ELONGATED HYPOCOTYL 5 (HY5)* transcription factor is a major positive regulator of photomorphogenesis both in visible (Lee *et al.*, 2007) and UV-B light (Ulm *et al.*, 2004; Brown *et al.*, 2005; Oravecz *et al.*, 2006; Binkert *et al.*, 2014). *hy5* mutants are largely impaired in UV-B-responsive gene expression and the accumulation of UV-B-protective flavonoid pigments, leading to reduced UV-B tolerance and survival (Brown *et al.*, 2005; Oravecz *et al.*, 2006; Stracke *et al.*, 2010). UV-B irradiation was shown to rapidly induce *HY5* gene expression (Ulm *et al.*, 2004; Brown & Jenkins, 2008; Binkert *et al.*, 2014; Binkert *et al.*, 2016) and the accumulation of *HY5* protein in the nucleus (Oravecz *et al.*, 2006).

UV-B penetrates rather poorly into tissues below the epidermis. Indeed, leaf epidermal transmittance of UV-B is less than 10%, measured in many different species under various circumstances (Robberecht *et al.*, 1980; Day *et al.*, 1993; Markstadter *et al.*, 2001; Qi *et al.*, 2003; Nybakken *et al.*, 2004). UVR8 is expressed ubiquitously in different organs of mature Arabidopsis (Rizzini *et al.*, 2011), but the precise distribution pattern and the accumulation level of the photoreceptor in various tissues have not yet been investigated. It follows that it is not understood how the action of UVR8 in different tissues/organs is integrated to regulate complex physiological responses as hypocotyl growth inhibition or leaf size, and how the strongly varying UV-B intensities in different tissues modulate UVR8-dependent signalling.

Correspondence: András Viczián. E-mail: viczian.andras@brc.mta.hu

Here, we characterized the spatio-temporal aspects of UV-B-induced, UVR8-mediated signalling to provide insight into the molecular mechanism mediating signal integration between different tissues/organs. We firstly determined the distribution pattern and level of YFP-UVR8 under the control of its own promoter. Next, we characterized to what extent UV-B-induced physiological and molecular responses are mediated by tissue-autonomous and/or inter-tissue signalling in transgenic lines that expressed the photoreceptor in a tissue-specific fashion. Our data suggest that UVR8 responses are mediated partly by tissue-autonomous signalling, but proper regulation of hypocotyl growth inhibition and establishment of UV-B tolerance require either UVR8 action in different tissues and/or inter-tissue signalling.

MATERIALS AND METHODS

Molecular cloning

The coding region of *YFP* and *UVR8* was cloned into the pPCV812 plasmid (Bauer *et al.*, 2004) as *SmaI-EcoRI* and *EcoRI-SacI* fragments, respectively. The *MERISTEM LAYER 1* (*ProML1*), *SUCROSE/H⁺ SYMPORTER 2* (*ProSUC2*) and *CHLOROPHYLL A/B BINDING PROTEIN 3* (*ProCAB3*) promoter fragments were cloned as described by Kirchenbauer *et al.* (2016) whereas the *ProUVR8* was inserted as a 2569 bp *SallI-BamHI* fragment including the 5' leader sequence. The coding sequence of the β -glucuronidase (*GUS*) as a *SmaI-XhoI* fragment (Adam *et al.*, 1995), *GFP* as a *XhoI-ClaI* fragment and *NLS* as a *ClaI-SacI* fragment (Wolf *et al.*, 2011) were cloned into the pPCVB812 binary vector (Bauer *et al.*, 2004) resulting in *GUS-GFP-NLS pPCVB*. This vector was digested with *HindIII* and *SmaI* restriction enzymes and the *ProHY5* (Oravecz *et al.*, 2006) was inserted as a *HindIII-StuI* fragment replacing the *Pro35S* promoter. *ProELIP2* and *ProPRR9* were cloned as 2772 bp (*BamHI-XbaI*) and 1324 bp (*BamHI-SmaI*) fragments including the 5' leader sequences, respectively. Cloning of *ProHY5:HY5-GFP* was described in detail by Kirchenbauer *et al.* (2016).

Plant material

Throughout the study, we used the *Arabidopsis thaliana* L (Heynh.) *uvr8-6* null mutant (Favory *et al.*, 2009), with the Columbia accession as wild type (WT) control. We raised 10 independent transgenic lines per construct and selected those which segregated the transgene as a single Mendelian trait. At least three independent lines were studied, and comparable results are presented. *Arabidopsis* transformation, principles of selection and handling of transgenic lines were described earlier in detail (Kirchenbauer *et al.*, 2016).

Seedling growth conditions and light treatments

Seeds were surface sterilized and subsequently stratified for 72 h in the dark (4°C) on ½ Murashige and Skoog (MS) medium (Sigma-Aldrich, Budapest, Hungary) containing 1% sucrose and 0.8% agar. For microscopic analysis, the seedlings

were grown in 12 h white light (WL, 80 $\mu\text{mol m}^{-2} \text{s}^{-1}$)/12 h dark at 22°C for 6 days (MLR-350, Sanyo, Gallenkamp, UK) and then placed under continuous white light supplemented with UV-B for 16 h at 22°C. White light was produced by PHILIPS TL-D 18 W/33-640 tubes (10 $\mu\text{mol m}^{-2} \text{s}^{-1}$). Non-damaging photomorphogenic (low-fluence) UV-B was produced by PHILIPS ULTRAVIOLET-B TL20W/01RS tubes (1.5 $\mu\text{mol m}^{-2} \text{s}^{-1}$). To modulate UV-B light, we used 3-mm-thick transmission cut-off filters of the WG series (Schott, Mainz, Germany), as described previously (Ulm *et al.*, 2004). UV-B treated seedlings (+UV-B) were covered with WG305 filter with half-maximal transmission at 305 nm, whereas non-UV-B irradiated control seedlings were covered with WG385 filter with half-maximal transmission at 385 nm (–UV-B) as applied in work published earlier (Oravecz *et al.*, 2006; Favory *et al.*, 2009; Rizzini *et al.*, 2011). UV-B was measured with a VLX-3 W UV light meter equipped with a CX-312 sensor (Vilber Lourmat, Eberhardzell, Germany), and the visible part was measured with an LI-250 Light Meter (Li-Cor, Lincoln, NE, USA). For hypocotyl and cotyledon measurements, seedlings were grown for 3 days in light/dark chambers before being exposed to continuous WL supplemented with UV-B for 4 days or 5 days.

Microscopy techniques

Confocal laser scanning microscopy (CLSM) settings and quantification of nuclear fluorescence were described in detail by Kirchenbauer *et al.* (2016)

Flavonoid detection using confocal laser scanning microscopy

Seeds were stratified and germinated as described above. Seedlings were grown for 2 days in 12 h light/12 h dark chambers and were placed under 1.5 $\mu\text{mol m}^{-2} \text{s}^{-1}$ WL supplemented with 1.5 $\mu\text{mol m}^{-2} \text{s}^{-1}$ UV-B light for 4 days. Seedlings treated with UV-B were covered with a WG305 filter, whereas the negative controls (–UV-B) were covered with WG385. Prior to microscopic analysis, seedlings were incubated in 0.1% (w/v) Naturstoffreagenz A (DPBA, Sigma-Aldrich) in 0.15 M phosphate buffer (pH 6.8) in the dark. After 15 min incubation time, DPBA was removed by exchanging the buffer for fresh phosphate buffer twice. CLSM was used to detect DPBA-flavonoid specific fluorescence (488 nm laser; pinhole: 200 μm ; spectral emission detector: 501–601 nm).

Hypocotyl length and cotyledon area measurements

Measurements of hypocotyl length and cotyledon area were performed as described earlier (Adam *et al.*, 2013). At least 40 seedlings (hypocotyl length) or 100 cotyledons were measured for each line and each treatment. Ratios of UV-B treated/non-treated hypocotyl lengths and cotyledon areas were calculated in each experiment. Experiments were repeated at least three times. The calculated ratio values were

averaged, and the standard error values of the means were obtained and plotted.

Protein isolation and western blot

Preparation of plant protein extracts and western blotting were described by Bauer *et al.* (2004). Application of anti-UVR8, anti-ACTIN antibodies and signal processing were also described earlier (Heijde & Ulm, 2013; Medzihradsky *et al.*, 2013). All protein extraction and western blotting were repeated three times, and a representative image is presented. Signal quantification was made using Image J software (NIH).

Determination of transcript levels

Total RNA isolation, cDNA synthesis and quantitative RT-PCR analysis were performed as described by Feher *et al.* (2011).

Propagation and UV-B treatment of adult plants for phenotype analysis and chlorophyll determination

Arabidopsis seeds were sown on soil, stratified for three days at 4 °C and then grown in a climate-controlled growth chamber (Grobank, CLF Plant Climatics, Wertingen, Germany) in short days conditions (8 h light/16 h dark) under WL (120 $\mu\text{mol m}^{-2} \text{s}^{-1}$) or WL supplemented with UV-B at 22 °C. The visible part was measured with an LI-250 Light Meter (Li-Cor). The light conditions in the chambers were set following the general guidelines described by Aphalo *et al.* (2012), and the full spectra of the applied light were analysed with a QE65000 spectrometer (Ocean Optics, Dunedin, FL, USA) (Fig. S1). We used white fluorescent tubes (Osram L18W) and the same type narrowband UV-B tubes, what were used in the seedling irradiation treatments (TL20W/01RS, Philips) without plastic filtering. The applied UV-B fluence rates (2 or 12 $\mu\text{mol m}^{-2} \text{s}^{-1}$) were comparable to the natural values measured in Szeged, Hungary on an average sunny summer day (7–15 $\mu\text{mol m}^{-2} \text{s}^{-1}$ between 11:00 and 13:00 CET on 09.06.2010.). UV-B was measured with a VLX-3 W UV light meter equipped with a CX-312 sensor (Vilber Lourmat). Rosette diameter was quantified in images of 7-week-old plants using ImageJ. Three repetitions of each experiment were performed using two independent lines for the tissue-specific lines. At least four plants were measured in each repetition for each genotype and independent line. Determination of chlorophyll levels was described earlier (Porra *et al.*, 1989).

RESULTS

Expression of the *ProUVR8:YFP-UVR8* transgene is restricted to epidermal and mesophyll cells

To address where UVR8 is expressed, we generated transgenic lines expressing the YFP-UVR8 fusion protein under the control of its own promoter in a *uvr8* null mutant background and determined its expression pattern by using

CLSM. We found that the *UVR8* promoter drives the expression of YFP-UVR8 in the epidermal and, to a lesser extent, the mesophyll/subepidermal cells of cotyledons and hypocotyls (Figs 1a–c, S2–S4). Accumulation of the YFP-UVR8 fusion protein was below detection level in the vascular bundles. But it should be noted that the YFP-UVR8 amount corresponded to ~10% of the native UVR8 protein detected in WT seedlings (Fig. 2a) and that we did not identify any *ProUVR8:YFP-UVR8* line with higher YFP-UVR8 protein amounts.

Characterization of transgenic lines expressing YFP-UVR8 in selected tissues

To assess the function of UVR8 located in different tissues, we expressed YFP-UVR8 in the *uvr8* mutant background under the control of *ProML1*, *ProSUC2* and *ProCAB3* promoters that have already been used in numerous studies to express proteins of interest in epidermal, companion and mesophyll cells, respectively (Mitra *et al.*, 1989; Sessions *et al.*, 1999; Srivastava *et al.*, 2008; Kirchenbauer *et al.*, 2016). Figures 1d–i and S2–S4 demonstrate that the *ProML1* drives the expression of YFP-UVR8 selectively in epidermal cells, whereas *ProCAB3* in the sub-epidermal (mesophyll) cells of cotyledons and hypocotyls. As expected, no activity of these promoters was detected in the vascular bundles. By contrast, *ProSUC2* expressed YFP-UVR8 in the vasculature and sub-epidermal cells of cotyledons and hypocotyls (Figs 1j–l and S2–S4). Western blot analysis showed that the total amount of YFP-UVR8 in *ProML1:YFP-UVR8* was ~5%, in *ProSUC2:YFP-UVR8* ~25% and in *ProCAB3:YFP-UVR8* 75% of the amount of endogenous UVR8 in WT seedlings (Fig. 2a). To facilitate direct comparison of the level of YFP-UVR8 in different cell types, we monitored its accumulation by CLSM. The amount of YFP-UVR8 was (1) comparable in the epidermal cells of *ProUVR8:YFP-UVR8* and *ProML1:YFP-UVR8*; (2) about four to fivefold lower in the mesophyll cells of *ProUVR8:YFP-UVR8* as compared to *ProCAB3:YFP-UVR8* and about the same in *ProSUC2:YFP-UVR8* (Fig. S5). It was not feasible to compare its accumulation by this method in the vascular bundles.

Complementation of seedling phenotypes of the *uvr8-6* mutant by tissue-specific expression of YFP-UVR8

To assess the function of UVR8 in different tissues, we measured typical photomorphogenic responses such as inhibition of hypocotyl elongation and expansion of cotyledons, of the various transgenic seedlings exposed to UV-B irradiation. Figure 2b shows that supplemental narrowband UV-B inhibited hypocotyl growth in the wild-type seedlings, whereas the *uvr8* mutant seedlings were much less responsive, in agreement with previous results (Favory *et al.*, 2009). All transgenic seedlings, except *ProSUC2:YFP-UVR8*, showed pronounced UV-B-induced hypocotyl growth inhibition, but did not fully complement the phenotype of the *uvr8* mutant (Fig. 2b). We

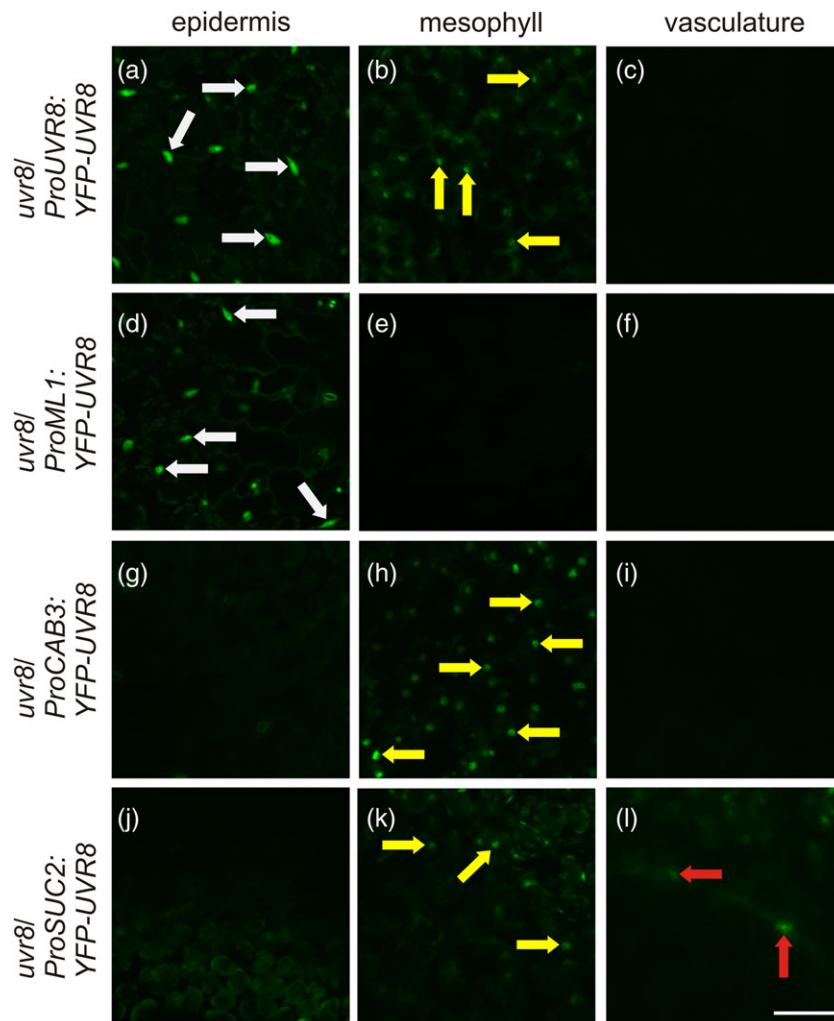


Figure 1. Tissue-specific expression of YFP-UVR8 in the cotyledons of transgenic *uvr8-6* seedlings. Localization of the YFP-UVR8 fusion protein was monitored by CLSM in the cotyledons of seedlings grown in constant WL supplemented with UV-B. To facilitate comparison of the expression levels of YFP-UVR8 in the examined transgenic lines, images representing the same tissue were obtained using identical microscope settings. The epidermis (a, d, g, j), the sub-epidermal mesophyll cells (b, e, h, k) and the vasculature (c, f, i, l) of seedlings expressing *ProUVR8:YFP-UVR8*, (a, b, c) or *ProML1:YFP-UVR8* (d, e, f) or *ProCAB3:YFP-UVR8* (g, h, i) or *ProSUC2:YFP-UVR8* (j, k, l) were examined. White arrows mark positions of selected nuclei in the epidermis, yellow arrows point to nuclei in the mesophyll, whereas red arrows indicate nuclei/cells in the vasculature. Scale bar = 50 μ m.

also measured the changes of cotyledon area caused by UV-B irradiation. Figure 2c illustrates that UV-B irradiation decreased the cotyledon size of the *uvr8*, *ProCAB3:YFP-UVR8* and the *ProSUC2:YFP-UVR8* seedlings, whereas the same UV-B treatment slightly increased the cotyledon size in the *ProUVR8:YFP-UVR8*, *ProML1:YFP-UVR8* and wild-type plants.

The above results indicate that (1) the YFP-UVR8 fusion protein is a functional photoreceptor, confirming previous reports (Brown *et al.*, 2005; Kaiserli & Jenkins, 2007; Huang *et al.*, 2014; Binkert *et al.*, 2016); (2) UVR8 signalling contributes to UV-B-induced inhibition of hypocotyl growth both in the epidermal and mesophyll cells; (3) UVR8 expression in the epidermis is necessary for proper cotyledon expansion under UV-B light; and (4) YFP-UVR8 expressed in vascular bundles plays a very limited role, if any, in regulating hypocotyl growth and cotyledon expansion (Table S1).

The UV-B-induced, UVR8-regulated induction of *HY5* is tissue autonomous

Increase in the mRNA level and nuclear accumulation of the key UV-B signal transduction component *HY5* are among the early steps of the UV-B-induced signalling cascade initiated by UVR8 (Ulm *et al.*, 2004; Brown *et al.*, 2005; Oravec *et al.*, 2006). To examine the tissue specificity of these responses, we introduced the *ProHY5:HY5-GFP* (to determine the cell-specific accumulation of *HY5* protein) and *ProHY5:GUS-GFP-NLS* (to determine the cell-specific induction of *HY5* transcription) reporters into transgenic *uvr8* mutant lines expressing YFP-UVR8 in different tissues. Figure 3 demonstrates that (1) the abundance of *HY5-GFP* was low in seedlings grown in white light, and (2) UV-B irradiation promoted accumulation of *HY5-GFP* only in those cells which also contained detectable amounts of YFP-UVR8. Similarly,

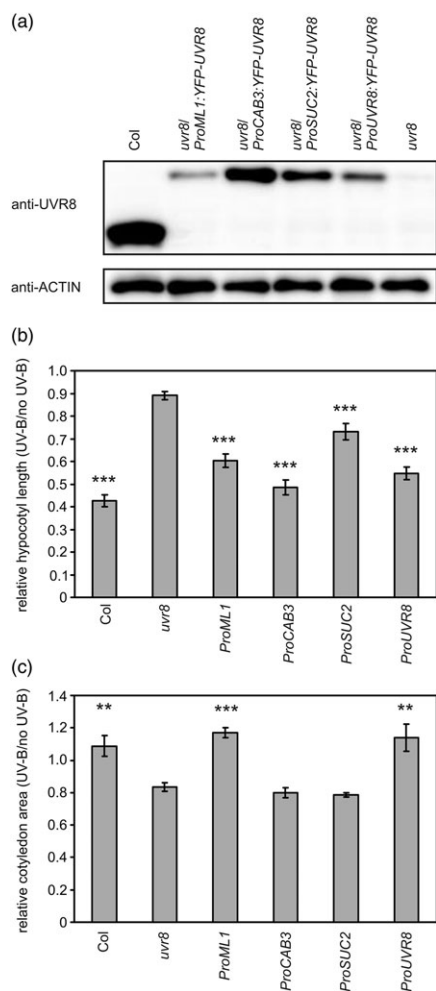


Figure 2. Expression and mutant phenotype complementation of YFP-UVR8 in *uvr8-6*. (a) Determination of endogenous UVR8 and YFP-UVR8 protein levels. Total protein extract was isolated from 4-day-old seedlings grown under constant WL supplemented with UV-B. The proteins were detected using UVR8-specific antibody (anti-UVR8). The blot was reprobed with anti-ACTIN antibody as loading control. (b) Effect of UV-B on hypocotyl length. Hypocotyl lengths of seedlings irradiated with constant WL supplemented with (UV-B) or without (no-UV-B) UV-B for 4 days were measured and relative hypocotyl lengths (UV-B/no-UV-B) were calculated. Each measurement was repeated 3 times; error bars represent standard error of the mean. Lines: Col = Columbia wild type; *uvr8* = *uvr8-6* mutant, *ProUVR8* = *ProUVR8:YFP-UVR8*; *ProML1* = *ProML1:YFP-UVR8*; *ProCAB3* = *ProCAB3:YFP-UVR8*; *ProSUC2* = *ProSUC2:YFP-UVR8*. Each transgene is expressed in the *uvr8-6* background. Asterisks mark lines that display significant differences as compared with the *uvr8* mutant line calculated by the Student's *t*-test (significance: * $P < 0.05$, ** $P < 0.01$, *** $P < 0.005$). (c) Effect of UV-B on cotyledon expansion. Cotyledon areas of seedlings irradiated with constant WL supplemented with (UV-B) or without (no UV-B) UV-B were measured, and relative cotyledon areas (UV-B/no UV-B) are plotted here. Each measurement was repeated 3 times; error bars represent standard error of the mean. Lines: Col = Columbia wild type; *uvr8* = *uvr8-6* mutant, *ProUVR8* = *ProUVR8:YFP-UVR8*; *ProML1* = *ProML1:YFP-UVR8*; *ProCAB3* = *ProCAB3:YFP-UVR8*; *ProSUC2* = *ProSUC2:YFP-UVR8*. Each transgene is expressed in the *uvr8-6* background. Asterisks mark lines that display significant differences as compared with the *uvr8* mutant line calculated by the Student's *t*-test (significance: * $P < 0.05$, ** $P < 0.01$, *** $P < 0.005$).

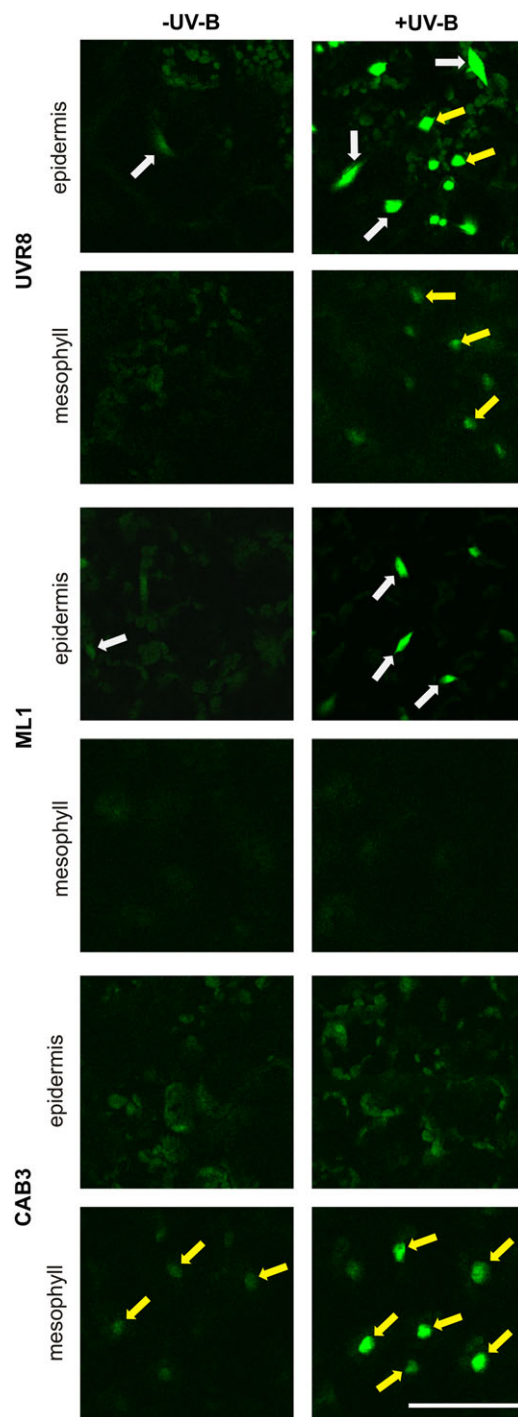


Figure 3. UV-B induction of *ProHY5:HY5-GFP* in the cotyledon cells of transgenic lines expressing YFP-UVR8 in different tissues. *ProHY5:HY5-GFP* was introduced into transgenic *uvr8* lines expressing *ProUVR8:YFP-UVR8* (UVR8), *ProML1:YFP-UVR8* (ML1) or *ProCAB3:YFP-UVR8* (CAB3). Localization of the HY5-GFP fusion protein was monitored by CLSM in the epidermis and mesophyll cells of the cotyledon of 7-day-old seedlings irradiated with constant WL supplemented with UV-B (+UV-B) or not supplemented (-UV-B). Identical microscope settings were used to allow determination of the difference between the visual signals of the +UV-B and -UV-B image pairs. White arrows mark the positions of selected nuclei in the epidermis; yellow arrows indicate nuclei in the mesophyll. Scale bar = 50 μ m.

we found that the UVR8-dependent induction of *HY5* transcription is also restricted to YFP-UVR8-containing cells (Fig. S6). Thus, our results indicate that regulation of the expression of *HY5* by UVR8 is a tissue-autonomous response.

UV-B induction of the transcription of *HY5*-dependent and -independent genes is controlled by UVR8 in a tissue-autonomous fashion

To get more insight into the tissue-related organization of UVR8 signalling, we also introduced the *ProELIP2:GUS-GFP-NLS* and *ProPRR9:GUS-GFP-NLS* transgenes into the *ProUVR8:YFP-UVR8*, *ProML1:YFP-UVR8* and *ProCAB3:YFP-UVR8* expressing lines. The *EARLY LIGHT-INDUCED PROTEIN 2 (ELIP2)* is involved in the photoprotection of thylakoid membranes (Hutin *et al.*, 2003). UV-B irradiation induces accumulation of *ELIP2* mRNA (Ulm *et al.*, 2004; Feher *et al.*, 2011), and this response requires functional UVR8 and *HY5* (Fig. S7) (Oravec *et al.*, 2006; Favory *et al.*, 2009). Figure 4 demonstrates that the activity of *ProELIP2* is low in white light, and that UV-B irradiation strongly enhances its activity only in those cells which also contain detectable amounts of YFP-UVR8, indicating that the photoreceptor regulates *HY5*-dependent expression of *ELIP2* in a tissue-autonomous fashion.

PSEUDO-RESPONSE REGULATOR 9 (PRR9) is a component of the plant circadian clock (Nakamichi *et al.*, 2005). UV-B-induction of *ProPRR9* depends on UVR8 (Feher *et al.*, 2011), but it is independent of *HY5* (Fig. S7). In contrast to the *HY5* and *ELIP2* promoters, *ProPRR9* was active in the sub-epidermal cells of cotyledons in transgenic plants grown in white light. UV-B strongly induced *ProPRR9* activity only in those sub-epidermal cells that contained detectable amounts of YFP-UVR8 (Fig. S8). Elevated expression of *ProPRR9:GUS-GFP-NLS* was not detectable in the epidermis of *ProML1:YFP-UVR8* and *ProUVR8:YFP-UVR8* lines, although these cells express YFP-UVR8.

UVR8-dependent flavonoid accumulation occurs in a tissue-autonomous fashion

DPBA forms complexes with flavonoid compounds, which can be visualized by CLSM (Schnitzler *et al.*, 1996; Hutzler *et al.*, 1998; Peer *et al.*, 2001). We applied an irradiation protocol which allowed detectable accumulation of flavonoids under supplemental UV-B in wild-type but not in *uvr8* seedlings. We detected the highest level of UV-B-induced flavonoid accumulation on the inner side of the adaxial epidermal cells in WT seedlings (Fig. 5), as previously reported (Hutzler *et al.*, 1998; Agati *et al.*, 2011). Moreover, all YFP-UVR8-expressing lines accumulated flavonoids UV-B-dependently, with a similar accumulation pattern but to lower levels than WT.

Adult plants require UVR8 in the mesophyll cells for proper acclimation and survival under UV-B

UVR8 plays a role not only at the seedling stage but also in acclimation to UV-B of adult plants (Favory *et al.*, 2009). We

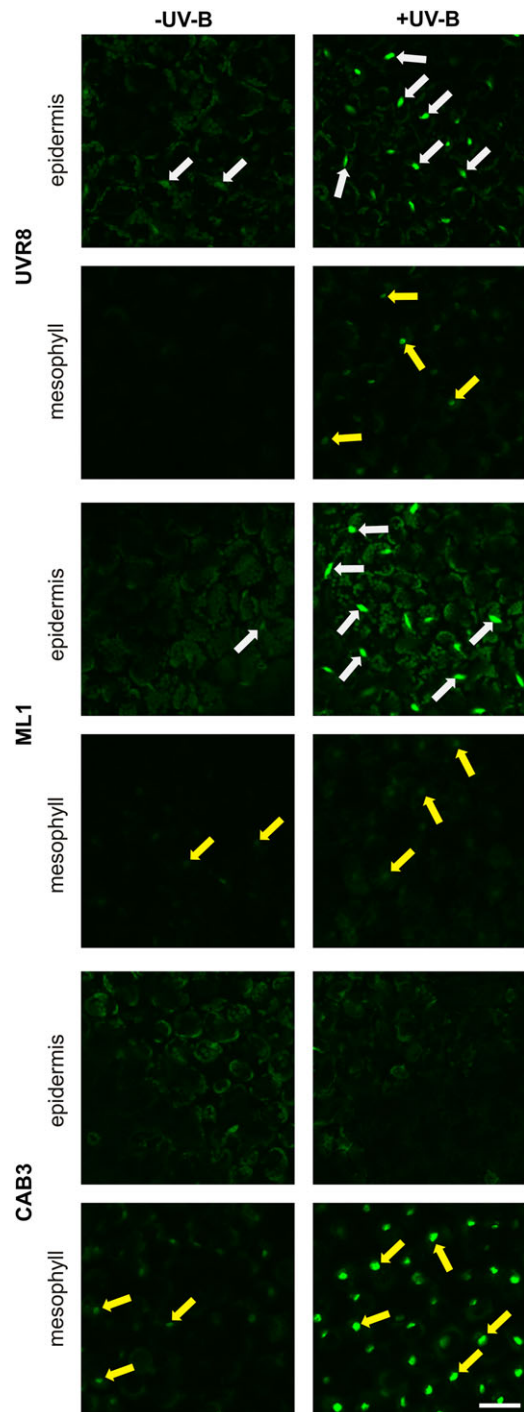


Figure 4. UV-B induction of *ProELIP2:GUS-GFP-NLS* in the cotyledon cells of transgenic lines expressing YFP-UVR8 in different tissues. *ProELIP2:GUS-GFP-NLS* was introduced into transgenic *uvr8-6* lines expressing *ProUVR8:YFP-UVR8* (UVR8), *ProML1:YFP-UVR8* (ML1) or *ProCAB3:YFP-UVR8* (CAB3). Localization of the GUS-GFP-NLS fusion protein was monitored by CLSM in the epidermis and mesophyll cells of the cotyledon of 7-day-old seedlings irradiated with constant WL supplemented with UV-B (+UV-B) or not supplemented (–UV-B). Identical microscope settings were used to allow determination of the difference between the visual signals of the +UV-B and –UV-B image pairs. White arrows mark the positions of selected nuclei in the epidermis; yellow arrows indicate nuclei in the mesophyll. Scale bar = 50 μ m.

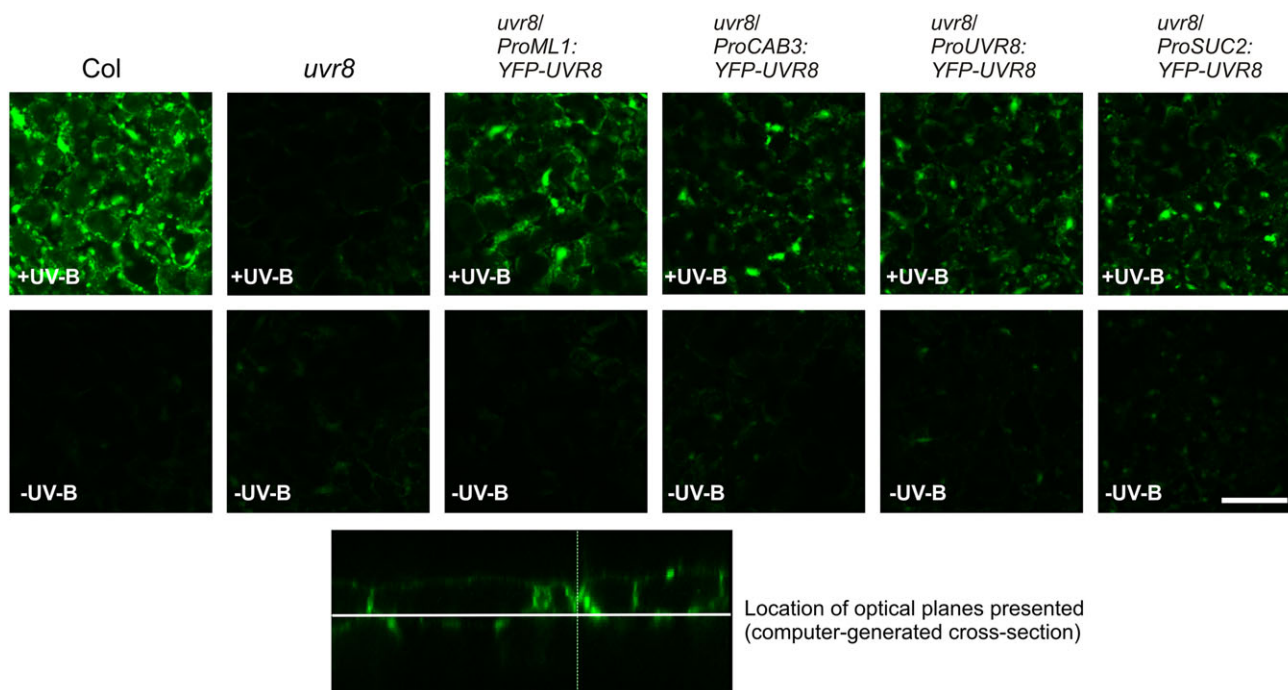


Figure 5. UV-B-induced flavonoid accumulation in the epidermis is regulated by UVR8 localized in both the epidermis and mesophyll cells. Three-day-old seedlings were grown under WL supplemented with weak UV-B for 4 days and were covered with WG305 (+UV-B) or with WG385 (–UV-B) filter. After incubation with DPBA, flavonoids were visualized (green colour) using CLSM. All images were taken using the same microscope settings. The focal plane was set to the bottom zone of the adaxial epidermis, where the highest signal was obtained (see bottom panel). Scale bar = 50 μm .

examined 7-week-old plants expressing YFP-UVR8 in different tissues and found that all plants developed equally without UV-B (Fig. 6a). Weak supplemental UV-B triggered rosette growth inhibition and shortening of petioles in the wild-type plants, whereas the *uvr8-6* mutant showed a very limited rosette growth reduction and developed light green leaves, indicating that this dose of UV-B elicited mainly UVR8 photoreceptor-mediated photomorphogenic responses (Fig. 6a). Thus, *uvr8* mutants are hyposensitive to UV-B considering UV-B-induced photomorphogenesis and acclimation, as previously reported (Favory *et al.*, 2009). Transgenic lines expressing YFP-UVR8 displayed WT-like acclimation (Fig. 6a), with comparable rosette development (Fig. 6b) and chlorophyll accumulation (Fig. 6c), except for the *ProCAB3:YFP-UVR8* plants, which had small rosettes (Fig. 6b) and accumulated chlorophyll to higher levels (Fig. 6c).

Stronger supplemental UV-B was lethal to *uvr8* mutants that, in contrast to wild type, were not able to acclimate to UV-B (Fig. 6a). Thus, under these conditions, the effect of UV-B acclimation on UV-B tolerance can be assayed. Next to wild type, also the *ProUVR8:YFP-UVR8* and *ProML1:YFP-UVR8* lines survived the higher UV-B levels but developed smaller rosettes. The *ProCAB3:YFP-UVR8* and *ProSUC2:YFP-UVR8* plants displayed a strong over-expression phenotype characteristic for plants producing high amounts of UVR8 under the control of constitutive promoters (Favory *et al.*, 2009; Heijde *et al.*, 2013; Fasano *et al.*, 2014). We found that these lines indeed over-expressed UVR8 in adult plants grown on soil as compared with WT (Fig. S9). Taken together, these results indicate that the expression of UVR8 in

subepidermal or epidermal tissues efficiently facilitates acclimation and survival under UV-B.

DISCUSSION

Analysis of transgenic *ProUVR8:YFP-UVR8* plants revealed the presence of the YFP-UVR8 fusion protein in the epidermal and sub-epidermal cells of cotyledons and hypocotyls of seedlings exposed to UV-B. However, in these lines, YFP-UVR8 accumulated to levels lower than endogenous UVR8; thus, we cannot exclude the presence of low amounts of UVR8 in the vascular tissues of WT seedlings. The fusion protein was biologically active, because the *ProUVR8:YFP-UVR8* transgenic seedlings and adult plants displayed partially or fully complemented UV-B responses. Thus, we assume that UVR8 signalling does not play a role in the vasculature, independently of the developmental stage.

ProML1:YFP-UVR8 displayed fully complemented UV-B-induced cotyledon expansion and partially restored hypocotyl growth inhibition, suggesting that epidermal UVR8 is critical for the regulation of these responses. *ProCAB3:YFP-UVR8* seedlings containing high levels of YFP-UVR8 in the subepidermal cells also displayed a partially complemented hypocotyl growth inhibition but a non-complemented cotyledon phenotype. The *ProSUC2:YFP-UVR8* line, despite the fact that it contained a relatively high amount of fusion protein, failed to complement cotyledon growth and displayed only a weak hypocotyl growth inhibition response (Table S1, Fig. 2). The latter could be the result of the UVR8 action in mesophyll cells rather than in the vasculature. Based on these data, we

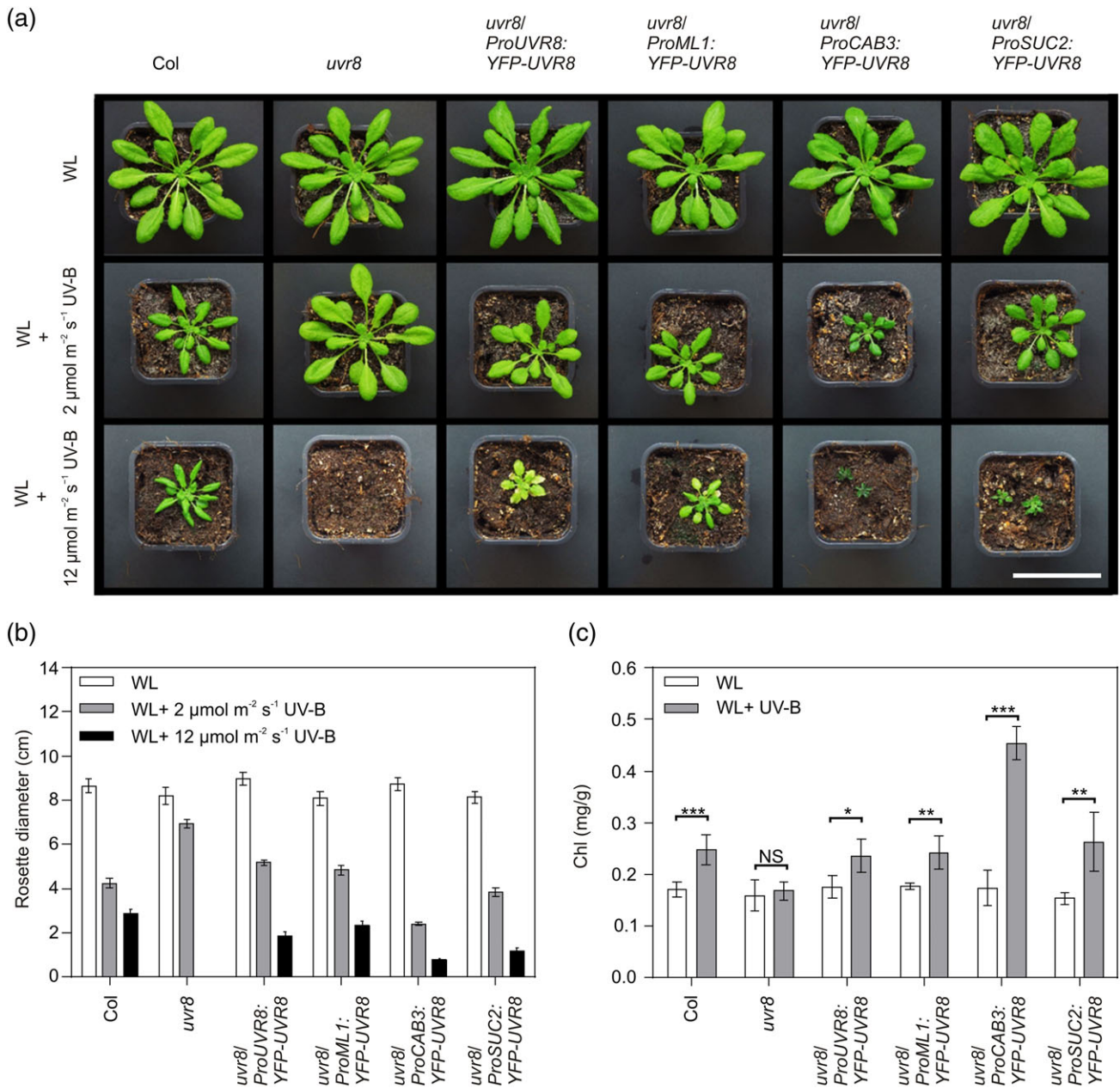


Figure 6. Effect of YFP-UVR8 expressed in different tissues of adult *Arabidopsis* plants. (a,b) Phenotypic characterization of adult plants grown under white light supplemented with UV-B. (a) Phenotypic characterization of 7-week-old *Arabidopsis* plants grown under white light (WL, $120 \mu\text{mol m}^{-2} \text{s}^{-1}$), WL plus UV-B at $2 \mu\text{mol m}^{-2} \text{s}^{-1}$ or WL plus UV-B at $12 \mu\text{mol m}^{-2} \text{s}^{-1}$ in short-day conditions. Scale bar: 5 cm. (b) Rosette diameter of 7-week-old plants grown as described above. Bars represent the average values calculated from three independent experiments. Error bars indicate the standard error of the mean. (c) Chlorophyll content of UV-B irradiated adult plants. Chlorophyll levels were determined from 7-week-old plants grown under white light or white light supplemented with UV-B ($1.5 \mu\text{mol m}^{-2} \text{s}^{-1}$) under short day conditions. Chl (mg/g) represents total chlorophyll content (mg/g fresh weight). Five plants were used as biological replicates for each line and light treatment. Error bars indicate standard error of the mean. Asterisks indicate values that are significantly different from WL treatment in the same genotype (Student's *t*-test, * $P < 0.05$, ** $P < 0.01$, *** $P < 0.005$). NS, no significance.

conclude that at the seedling stage, the primary sites of UV-B perception are the epidermis and, to a lesser extent, the mesophyll/sub-epidermal cells. The low penetration of UV-B into deeper layers of plant organs (Day *et al.*, 1993) lends further support to the above conclusion. The distinguished role of epidermis in regulating hypocotyl growth is not unique to UVR8 action, as similar data were reported for *phyA*

(Kirchenbauer *et al.*, 2016) *phyB* (Endo *et al.*, 2005; Kim *et al.*, 2016) and brassinosteroid signalling (Savaldi-Goldstein *et al.*, 2007). However, both Kirchenbauer *et al.* (2016) and Savaldi-Goldstein *et al.* (2007) concluded that exclusive action of *phyA* or brassinosteroid signalling in the epidermis is not sufficient to recapitulate full regulation of this response. Therefore, we assume that the UVR8-mediated inhibition of

hypocotyl growth is also mediated partly by the simultaneous action of UVR8 in various tissues and/or inter-tissue signalling.

Adult *ProCAB3:YFP-UVR8* and *ProSUC2:YFP-UVR8* plants having high levels of YFP-UVR8 in the mesophyll displayed an over-expression phenotype, whereas the phenotype of *ProUVR8:YFP-UVR8* plants was similar to WT when exposed to strong UV-B (Fig. 6). Although subepidermal/mesophyll cells also contain flavonoids (Agati *et al.*, 2011), we do not attribute the over-expression phenotype directly to the accumulation of flavonoids in these cell types. However, we assume that (1) UVR8 in the mesophyll is required for maintaining photosynthetic efficiency under elevated UV-B (Davey *et al.*, 2012) maybe by regulating the levels of the D1 and D2 core proteins, as described recently in *Chlamydomonas* (Tilbrook *et al.*, 2016), and that (2) this process needs UVR8 located in cells containing chloroplasts. As for proper rosette development, the phenotypes of the *ProML1:YFP-UVR8* and *ProUVR8:YFP-UVR8* lines suggest that together with the mesophyll UVR8, the action of epidermal UVR8 is still required. As for the *ProSUC2:YFP-UVR8* plant, it remains to be seen whether the activity of UVR8 in the vasculature contributes to the acclimation response, or it is due to *ProSUC2* promoter action in subepidermal cells. Taken together, we conclude that in mature plants, simultaneous signalling in the epidermal and mesophyll cells and/or inter-tissue signalling is required to optimize growth and development under UV-B.

UV-B-induced flavonoid accumulation both in the epidermis (*ProML1:YFP-UVR8* or *ProUVR8:YFP-UVR8*) and mesophyll cells (*ProCAB3:YFP-UVR8* or *ProSUC2:YFP-UVR8*) appears to be regulated by YFP-UVR8 located in the same tissue, that is, in a tissue-autonomous fashion (Fig. 5). However, at present, the contribution of inter-tissue signalling or transport of flavonoids (Buer *et al.*, 2007) in regulating their accumulation cannot be ruled out.

To provide a mechanistic explanation for UV-B-induced developmental responses, we examined the expression patterns of various genes shown to be regulated by UVR8. UV-B-induced transcription and accumulation of the key regulator HY5 were restricted to cells containing UVR8 (Figs 3 & S6). The phyA photoreceptor was also shown to regulate HY5 expression in a similar fashion (Kirchenbauer *et al.*, 2016). These data suggest that far-red and UV-B light regulated expression of HY5, probably an early, rate-limiting step of both signal transduction cascades, is mediated in a tissue-autonomous fashion by both photoreceptors. Similarly to HY5, the UV-B-induced expression of *ELIP2* which requires functional HY5 and that of *PRR9* whose expression is not regulated by HY5 occurs in a strictly tissue-autonomous way (Figs 4 & S8).

Taken together, we found no evidence at the molecular level that UVR8-signalling initiates signal crosstalk between different tissues. However, it was reported that UV-B irradiation of certain parts of the plants results in changes of gene expression in shielded organs, indicating that UV-B-induced inter-organ signalling can occur in higher plants (Casati & Walbot, 2004). Therefore, we hypothesize that inter-tissue signalling, mediated by yet unknown mobile compounds, contributes to the

manifestation of UVR8-regulated responses. For example, it was reported that HY5 regulates auxin signalling under different light treatments including UV-B irradiation (Cluis *et al.*, 2004; Sibout *et al.*, 2006; Hayes *et al.*, 2014; Vandebussche *et al.*, 2014). However, to unravel the molecular aspects of UVR8-modulated hormone signalling requires the development of new cellular markers.

ACKNOWLEDGEMENT

We thank Ferhan Ayaydin (Cellular Imaging Laboratory, Biological Research Centre, Szeged) for the help with CLSM. We also thank János Bindics and Kata Terecskei for having initiated the project. Work in Geneva, Switzerland was supported by the University of Geneva and a Swiss National Science Foundation grant (no. 31003A_153475) to R.U. The work in Szeged, Hungary was supported by two Hungarian Scientific Research Fund grants (OTKA, K-108559 and NN-110636); GINOP-2.3.2-15-2016-00001 and GINOP-2.3.2-15-2016-00015 grants to F.N. and a Bolyai János Research Scholarship of the Hungarian Academy of Sciences to A.V. Work in Edinburgh, UK was supported by a BBSRC grant BB/K006975/1 to F.N.

REFERENCES

- Adam E., Kircher S., Liu P., Merai Z., Gonzalez-Schain N., Horner M., ... *et al.* (2013) Comparative functional analysis of full-length and N-terminal fragments of phytochrome C, D and E in red light-induced signaling. *New Phytol* **200**(1), 86–96.
- Adam E., Kozma-Bognar L., Dallmann G. & Nagy F. (1995) Transcription of tobacco phytochrome-A genes initiates at multiple start sites and requires multiple cis-acting regulatory elements. *Plant Mol Biol* **29**(5), 983–993.
- Agati G., Biricolti S., Guidi L., Ferrini F., Fini A. & Tattini M. (2011) The biosynthesis of flavonoids is enhanced similarly by UV radiation and root zone salinity in *L. vulgare* leaves. *J Plant Physiol* **168**(3), 204–212.
- Aphalo PJ, Albert A, Björn LO, McLeod A, Robson TM, Rosenqvist E. (eds.) 2012. Beyond the visible: a handbook of best practice in plant UV photobiology. COST Action FA0906 UV4growth. Helsinki: University of Helsinki, Department of Biosciences, Division of Plant Biology. ISBN 978-952-10-8362-4 (Paperback), 978-952-10-8363-1 (PDF). xxx + 176 pp.
- Bauer D., Viczian A., Kircher S., Nobis T., Nitschke R., Kunkel T., ... *et al.* (2004) Constitutive photomorphogenesis 1 and multiple photoreceptors control degradation of phytochrome interacting factor 3, a transcription factor required for light signaling in Arabidopsis. *Plant Cell* **16**(6), 1433–1445.
- Binkert M., Crocco C.D., Ekundayo B., Lau K., Raffelberg S., Tilbrook K., ... Ulm R. (2016) Revisiting chromatin binding of the Arabidopsis UV-B photoreceptor UVR8. *BMC Plant Biol* **16**, 42.
- Binkert M., Kozma-Bognar L., Terecskei K., De Veylder L., Nagy F. & Ulm R. (2014) UV-B-responsive association of the Arabidopsis bZIP transcription factor ELONGATED HYPOCOTYL5 with target genes, including its own promoter. *Plant Cell* **26**(10), 4200–4213.
- Brown B.A., Cloix C., Jiang G.H., Kaiserli E., Herzyk P., Kliebenstein D.J. & Jenkins G.I. (2005) A UV-B-specific signaling component orchestrates plant UV protection. *Proc Natl Acad Sci U S A* **102**(50), 18225–18230.
- Brown B.A. & Jenkins G.I. (2008) UV-B signaling pathways with different fluence-rate response profiles are distinguished in mature Arabidopsis leaf tissue by requirement for UVR8, HY5, and HYH. *Plant Physiol* **146**(2), 576–588.
- Buer C.S., Muday G.K. & Djordjevic M.A. (2007) Flavonoids are differentially taken up and transported long distances in Arabidopsis. *Plant Physiol* **145**(2), 478–490.
- Casati P. & Walbot V. (2004) Rapid transcriptome responses of maize (*Zea mays*) to UV-B in irradiated and shielded tissues. *Genome Biol* **5**(3), R16.
- Cloix C. & Jenkins G.I. (2008) Interaction of the Arabidopsis UV-B-specific signaling component UVR8 with chromatin. *Mol Plant* **1**(1), 118–128.

- Cluis C.P., Mouchel C.F. & Hardtke C.S. (2004) The Arabidopsis transcription factor HY5 integrates light and hormone signaling pathways. *Plant J* **38**(2), 332–347.
- Davey M.P., Susanti N.I., Wargent J.J., Findlay J.E., Paul Quick W., Paul N.D. & Jenkins G.I. (2012) The UV-B photoreceptor UVR8 promotes photosynthetic efficiency in *Arabidopsis thaliana* exposed to elevated levels of UV-B. *Photosynth Res* **114**(2), 121–131.
- Day T.A., Martin G. & Vogelmann T.C. (1993) Penetration of UV-B radiation in foliage: evidence that the epidermis behaves as a non-uniform filter. *Plant, Cell & Environment* **16**(6), 735–741.
- Endo M., Nakamura S., Araki T., Mochizuki N. & Nagatani A. (2005) Phytochrome B in the mesophyll delays flowering by suppressing FLOWERING LOCUS T expression in Arabidopsis vascular bundles. *Plant Cell* **17**(7), 1941–1952.
- Fasano R., Gonzalez N., Tosco A., Dal Piaz F., Docimo T., Serrano R., ... Inze D. (2014) Role of Arabidopsis UV RESISTANCE LOCUS 8 in plant growth reduction under osmotic stress and low levels of UV-B. *Mol Plant* **7**(5), 773–791.
- Favory J.J., Stec A., Gruber H., Rizzini L., Oravecz A., Funk M., ... et al. (2009) Interaction of COP1 and UVR8 regulates UV-B-induced photomorphogenesis and stress acclimation in Arabidopsis. *EMBO J* **28**(5), 591–601.
- Feher B., Kozma-Bognar L., Kevei E., Hajdu A., Binkert M., Davis S.J., ... Nagy F. (2011) Functional interaction of the circadian clock and UV RESISTANCE LOCUS 8-controlled UV-B signaling pathways in *Arabidopsis thaliana*. *Plant J* **67**(1), 37–48.
- Galvao V.C. & Fankhauser C. (2015) Sensing the light environment in plants: photoreceptors and early signaling steps. *Curr Opin Neurobiol* **34**, 46–53.
- Hayes S., Velanis C.N., Jenkins G.I. & Franklin K.A. (2014) UV-B detected by the UVR8 photoreceptor antagonizes auxin signaling and plant shade avoidance. *Proc Natl Acad Sci U S A* **111**(32), 11894–11899.
- Heijde M., Binkert M., Yin R., Ares-Orpel F., Rizzini L., Van De Slijke E., ... et al. (2013) Constitutively active UVR8 photoreceptor variant in Arabidopsis. *Proc Natl Acad Sci U S A* **110**(50), 20326–20331.
- Heijde M. & Ulm R. (2013) Reversion of the Arabidopsis UV-B photoreceptor UVR8 to the homodimeric ground state. *Proc Natl Acad Sci U S A* **110**(3), 1113–1118.
- Hollosy F. (2002) Effects of ultraviolet radiation on plant cells. *Micron* **33**(2), 179–197.
- Huang X., Yang P., Ouyang X., Chen L. & Deng X.W. (2014) Photoactivated UVR8-COP1 module determines photomorphogenic UV-B signaling output in Arabidopsis. *PLoS Genet* **10**(3), e1004218.
- Hutin C., Nussaume L., Moise N., Moya I., Kloppstech K. & Havaux M. (2003) Early light-induced proteins protect Arabidopsis from photooxidative stress. *Proc Natl Acad Sci U S A* **100**(8), 4921–4926.
- Hutzler P., Fischbach R., Heller W., Jungblut T.P., Reuber S., Schmitz R., ... Schnitzler J.-P. (1998) Tissue localization of phenolic compounds in plants by confocal laser scanning microscopy. *Journal of Experimental Botany* **49**(323), 953–965.
- Jenkins G.I. (2014) The UV-B photoreceptor UVR8: from structure to physiology. *Plant Cell* **26**(1), 21–37.
- Kaiserli E. & Jenkins G.I. (2007) UV-B promotes rapid nuclear translocation of the Arabidopsis UV-B specific signaling component UVR8 and activates its function in the nucleus. *Plant Cell* **19**(8), 2662–2673.
- Kim J., Song K., Park E., Kim K., Bae G. & Choi G. (2016) Epidermal phytochrome B inhibits hypocotyl negative gravitropism non-cell autonomously. *Plant Cell* **28**(11), 2770–2785.
- Kirchenbauer D., Viczian A., Adam E., Hegedus Z., Klose C., Leppert M., ... Nagy F. (2016) Characterization of photomorphogenic responses and signaling cascades controlled by phytochrome-A expressed in different tissues. *New Phytol.* **211**(2), 584–98.
- Kliebenstein D.J., Lim J.E., Landry L.G. & Last R.L. (2002) Arabidopsis UVR8 regulates ultraviolet-B signal transduction and tolerance and contains sequence similarity to human regulator of chromatin condensation 1. *Plant Physiol* **130**(1), 234–243.
- Lee J., He K., Stolc V., Lee H., Figueroa P., Gao Y., ... Deng X.W. (2007) Analysis of transcription factor HY5 genomic binding sites revealed its hierarchical role in light regulation of development. *Plant Cell* **19**(3), 731–749.
- Markstadter C., Queck I., Baumeister J., Riederer M., Schreiber U. & Bilger W. (2001) Epidermal transmittance of leaves of *Vicia faba* for UV radiation as determined by two different methods. *Photosynth Res* **67**(1–2), 17–25.
- Medzhradszky M., Bindics J., Adam E., Viczian A., Klement E., Lorrain S., ... et al. (2013) Phosphorylation of phytochrome B inhibits light-induced signaling via accelerated dark reversion in Arabidopsis. *Plant Cell* **25**(2), 535–544.
- Mitra A., Choi H.K. & An G. (1989) Structural and functional analyses of *Arabidopsis thaliana* chlorophyll a/b-binding protein (cab) promoters. *Plant Mol Biol* **12**(2), 169–179.
- Morales L.O., Brosche M., Vainonen J., Jenkins G.I., Wargent J.J., Sipari N., ... Aphalo P.J. (2013) Multiple roles for UV RESISTANCE LOCUS8 in regulating gene expression and metabolite accumulation in Arabidopsis under solar ultraviolet radiation. *Plant Physiol* **161**(2), 744–759.
- Nakamichi N., Kita M., Ito S., Yamashino T. & Mizuno T. (2005) PSEUDO-RESPONSE REGULATORS, PRR9, PRR7 and PRR5, together play essential roles close to the circadian clock of *Arabidopsis thaliana*. *Plant Cell Physiol* **46**(5), 686–698.
- Nybakken L., Bilger W., Johanson U., Björn L.O., Zielke M. & Solheim B. (2004) Epidermal UV-screening in vascular plants from Svalbard (Norwegian Arctic). *Polar Biology* **27**(7), 383–390.
- Oravecz A., Baumann A., Mate Z., Brzezinska A., Molinier J., Oakeley E.J., ... Ulm R. (2006) CONSTITUTIVELY PHOTOMORPHOGENIC1 is required for the UV-B response in Arabidopsis. *Plant Cell* **18**(8), 1975–1990.
- Peer W.A., Brown D.E., Tague B.W., Mудay G.K., Taiz L. & Murphy A.S. (2001) Flavonoid accumulation patterns of transparent testa mutants of Arabidopsis. *Plant Physiol* **126**(2), 536–548.
- Porra R.J., Thompson W.A. & Kriedemann P.E. (1989) Determination of accurate extinction coefficients and simultaneous equations for assaying chlorophylls a and b extracted with four different solvents: verification of the concentration of chlorophyll standards by atomic absorption spectroscopy. *Biochimica et Biophysica Acta (BBA) – Bioenergetics* **975**(3), 384–394.
- Qi Y., Bai S., Vogelmann T.C., Heisler G.M. (2003). Penetration of UV-A, UV-B, blue, and red light into leaf tissues of pecan measured by a fiber optic microprobe system. *Proceedings of SPIE* Vol. 5156 Ultraviolet Ground- and Space-based Measurements, Models, and Effects III, edited by James R. Slusser, Jay R. Herman, Wei Gao. 281–290. doi:10.1117/12.506629. <http://proceedings.spiedigitallibrary.org/proceeding.aspx?articleid=768358>
- Rizzini L., Favory J.J., Cloix C., Faggionato D., O'Hara A., Kaiserli E., ... et al. (2011) Perception of UV-B by the Arabidopsis UVR8 protein. *Science* **332**(6025), 103–106.
- Robberecht R., Caldwell M.M. & Billings W.D. (1980) Leaf ultraviolet optical properties along a latitudinal gradient in the arctic-alpine life zone. *Ecology* **61**(3), 612–619.
- Savaldi-Goldstein S., Peto C. & Chory J. (2007) The epidermis both drives and restricts plant shoot growth. *Nature* **446**(7132), 199–202.
- Schnitzler J.-P., Jungblut T.P., Heller W., Kofferlein M., Hutzler P., Heinzmann U., ... Sandermann H. (1996) Tissue localization of u.v.-B-screening pigments and of chalcone synthase mRNA in needles of Scots pine seedlings. *The New Phytologist* **132**(2), 247–258.
- Sessions A., Weigel D. & Yanofsky M.F. (1999) The *Arabidopsis thaliana* MERISTEM LAYER 1 promoter specifies epidermal expression in meristems and young primordia. *Plant J* **20**(2), 259–263.
- Sibout R., Sukumar P., Hettiarachchi C., Holm M., Muday G.K. & Hardtke C.S. (2006) Opposite root growth phenotypes of hy5 versus hy5 hyh mutants correlate with increased constitutive auxin signaling. *PLoS Genet* **2**(11), e202.
- Srivastava A.C., Ganesan S., Ismail I.O. & Ayre B.G. (2008) Functional characterization of the Arabidopsis AtSUC2 Sucrose/H+ symporter by tissue-specific complementation reveals an essential role in phloem loading but not in long-distance transport. *Plant Physiol* **148**(1), 200–211.
- Stracke R., Favory J.J., Gruber H., Bartelniewoehner L., Bartels S., Binkert M., ... Ulm R. (2010) The Arabidopsis bZIP transcription factor HY5 regulates expression of the PFG1/MYB12 gene in response to light and ultraviolet-B radiation. *Plant Cell Environ* **33**(1), 88–103.
- Tilbrook K., Dubois M., Crocco C.D., Yin R., Chappuis R., Allouret G., ... Ulm R. (2016) UV-B perception and acclimation in *Chlamydomonas reinhardtii*. *Plant Cell* **28**(4), 966–983.
- Ulm R., Baumann A., Oravecz A., Mate Z., Adam E., Oakeley E.J., Schafer E. & Nagy F. (2004) Genome-wide analysis of gene expression reveals function of the bZIP transcription factor HY5 in the UV-B response of Arabidopsis. *Proc Natl Acad Sci U S A* **101**(5), 1397–1402.
- Vandenbussche F., Tilbrook K., Fierro A.C., Marchal K., Poelman D., Van Der Straeten D. & Ulm R. (2014) Photoreceptor-mediated bending towards UV-B in Arabidopsis. *Mol Plant* **7**(6), 1041–1052.
- Wolf I., Kircher S., Fejes E., Kozma-Bognar L., Schafer E., Nagy F. & Adam E. (2011) Light-regulated nuclear import and degradation of Arabidopsis phytochrome-A N-terminal fragments. *Plant Cell Physiol* **52**(2), 361–372.
- Yin R., Skvortsova M.Y., Loubery S. & Ulm R. (2016) COP1 is required for UV-B-induced nuclear accumulation of the UVR8 photoreceptor. *Proc Natl Acad Sci U S A* **113**(30), E4415–4422.

Received 4 July 2016; received in revised form 20 December 2016; accepted for publication 24 December 2016

SUPPORTING INFORMATION

Additional Supporting Information may be found in the online version of this article at the publisher's web-site:

Table S1. Complementation of *uvr8* phenotype by different transgenes.

Figure S1. Full spectra of the applied light in the GroBank growth chambers

Figure S2. Detection of YFP-UVR8 in the cotyledon

Figure S3. Detection of YFP-UVR8 in the upper part of the hypocotyl

Figure S4. Detection of YFP-UVR8 in the lower part of the hypocotyl.

Figure S5. Determination of YFP-UVR8 accumulation in certain tissues.

Figure S6. UV-B induction of *ProHY5:GUS-GFP-NLS* in the cotyledon cells of transgenic lines expressing YFP-UVR8 in different tissues.

Figure S7. The UV-B-specific messenger accumulation of *ELIP2* does whereas the accumulation of *PRR9* does not depend on *HY5*.

Figure S8. UVB induction of *ProPRR9:GUS-GFP-NLS* in the cotyledon cells of transgenic lines expressing YFP-UVR8 in different tissues.

Figure S9. Determination of endogenous and YFP-UVR8 protein levels in adult plants.